Fluorescent Probes Hot Paper

How to cite: *Angew. Chem. Int. Ed.* **2021**, *60*, 11335–11343
International Edition: doi.org/10.1002/anie.202015988
German Edition: doi.org/10.1002/ange.202015988

Covalent Probes for Aggregated Protein Imaging via Michael Addition

*Wang Wan, Yanan Huang, Qiuxuan Xia, Yulong Bai, Yuwen Chen, Wenhan Jin, Mengdie Wang, Di Shen, Haochen Lyu, Yuqi Tang, Xuepeng Dong, Zhenming Gao, Qun Zhao, Lihua Zhang, and Yu Liu**

Abstract: *Covalent chemical reactions to modify aggregated proteins are rare. Here, we reported covalent Michael addition can generally occur upon protein aggregation. Such reactivity was initially discovered by a bioinspired fluorescent color-switch probe mimicking the photo-conversion mechanism of Kaede fluorescent protein. This probe was dark with folded proteins but turned on red fluorescence (620 nm) when it non-covalently bound to misfolded proteins. Supported by the biochemical and mass spectrometry results, the probe chemo-selectively reacted with the reactive cysteines of aggregated proteins via covalent Michael addition and gradually switched to green fluorescence (515 nm) upon protein aggregation. Exploiting this Michael addition chemistry in the malachite green dye derivatives demonstrated its general applicability and chemical tunability, resulting in different fluorescence color-switch responses. Our work may offer a new avenue to explore other chemical reactions upon protein aggregation and design covalent probes for imaging, chemical proteomics, and therapeutic purposes.*

Introduction

Proteins fold into their defined 3-dimentional structures to acquire proper biological functions.[1] These structures revealed by X-ray crystallography and electron microscopy guide the design of non-covalent probes to regulate protein functions. Further exploration of the chemical reactivity of proteins has resulted in countless reaction types at their folded state (Figure 1).[2,3] The inherent nucleophilicity of amino acids enables chemoselective bioconjugations,[4] such as activated ester to react with lysine, maleimide to react with cysteine, and various protein chemical ligation methods.[5–7] The unique catalytic environment of enzymes or binding proteins offers vastly diverse covalent reactions, including acylation, 1,4-Michael addition, alkylation, carbamylation, and boronation etc.[8–10] These covalent reactions allow us to develop covalent probes targeting folded proteins, including fluorescent probes for bio-imaging, covalent drugs for therapeutic purposes,[11–16] and activity based probes for chemical proteomics[17–24] etc. Besides these naturally existing chemical reactivity, introduction of unnatural amino acids enormously broadens the horizon of chemical reactivity and enriches the bioorthogonal chemistry toolbox for selective bioconjugation and functionalization of folded proteins.[25–28]

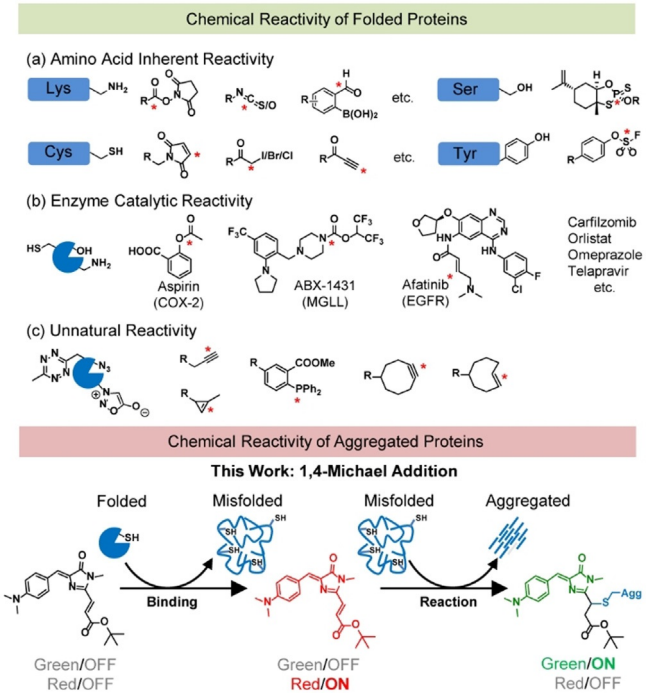

Figure 1. Chemical reactivity upon protein aggregation has not yet been fully explored. Defined structure and chemical reactivity of folded proteins facilitate the design of their covalent probes. Aggregated proteins are difficult to target via covalent modification due to the lack of reported chemical reactivity. This work reported 1,4-Michael addition can occur upon protein aggregation, yielding fluorescence color-switch probes.

Unlike folded proteins, the misfolded and aggregated proteins caused by genetic mutations, environmental stresses, chemical modifications, and ageing usually lose their 3-dimentioanl structures. Aberrant protein misfolding and aggregation in the cell often lead to numerous protein conformational diseases, such as neurodegeneration, metabolic disorders, cardiovascular diseases, and certain type of cancers.[29–32] Though conventionally considered to be structurally disordered, protein amyloid aggregation has been demonstrated to exhibit organized β-sheet stacked structures given the recent advances in the state-of-the-art microscopic

[*] W. Wan, Y. Huang, Q. Xia, Y. Bai, Y. Chen, W. Jin, M. Wang, D. Shen, H. Lyu, Y. Tang, Q. Zhao, L. Zhang, Y. Liu
CAS Key Laboratory of Separation Science for Analytical Chemistry, Dalian Institute of Chemical Physics, Chinese Academy of Sciences
457 Zhongshan Road, Dalian 116023 (China)
E-mail: liuyu@dicp.ac.cn
X. Dong, Z. Gao
The Second Hospital of Dalian Medical University
467 Zhongshan Road, Dalian 116044 (China)
Supporting information and the ORCID identification number(s) for the author(s) of this article can be found under: https://doi.org/10.1002/anie.202015988.

methods.[33] The structural information provides blueprint to design non-covalent dyes and sensors that selectively bind to amyloid aggregated proteins.[34] Organic dyes, like Thioflavin T, Congo Red, carbazoles, perylenes, and their derivatives have been demonstrated to selectively bind to amyloid precursors and fibrils.[35] In particular, Tang,[36] Zhu,[37] and Hong[38] et al. pioneered the design of AIEgens to report on amyloid and unfolded proteins during protein phase separation. Materials based probes, such as luminescent polymers, quantum dots, and nanoparticles opened new avenues for amyloid sensors.[39,40] Mirica[41] and Marti[42] et al. bridged the gap of organic dyes and inorganic materials by using organometallic complexes to probe amyloid proteins. These probes target protein amyloids via non-covalent intercalation into the intermolecular space of amyloid aggregates. Dyes like SYPRO orange and PROTEOSTAT that bind to amorphous protein aggregates of no defined structure were less reported.

While much light has been shed on the non-covalent probes for aggregated proteins, covalent probes targeting aggregated proteins have not been generally reported. This is probably due to the fact that the local chemical reactivity within aggregated proteins has not been fully explored. Recently, Zhang[43,44] and Hong[45] et al. embarked on the survey of the physical environment inside aggregated proteins, but their work primarily revealed the changes in polarity and viscosity upon protein aggregation using environment-sensitive probes. However, it still remains elusive how chemically reactive proteins are at their aggregated state. Therefore, current powerful chemical sensing and bioconjugation strategies[46–48] may provide hints to address this question.

In this work, we reported 1,4-Michael addition reaction can occur upon protein aggregation, which is useful to develop covalent probes for bioconjugation and imaging purposes (Figure 1). Such chemical reactivity was discovered by a bio-inspired fluorescent color-switch probe. This probe exhibited no fluorescence with folded proteins, red fluorescence in misfolded proteins, and green fluorescence in aggregated proteins. Mass spectrometry analyses revealed the fluorescence color-switch property was induced by chemoselective covalent Michael addition with cysteine residues that were reactive upon protein aggregation. We further exploited this chemistry to develop other fluorogenic color-switch probes and demonstrate its chemical tunability. The transmission electron microscopic images and protein proteolytic resistance results suggested that the compactness of aggregated proteins influenced their chemical reactivity. Last, we utilized this chemistry to selectively visualize aggregated proteome in stressed live cells.

Results and Discussion

Fluorescent Color-Switch Probe upon Protein Aggregation

Our initial hypothesis of the presence of chemical reactivity inside aggregated proteins was made on the basis of a fluorescent color-switch probe upon protein aggregation

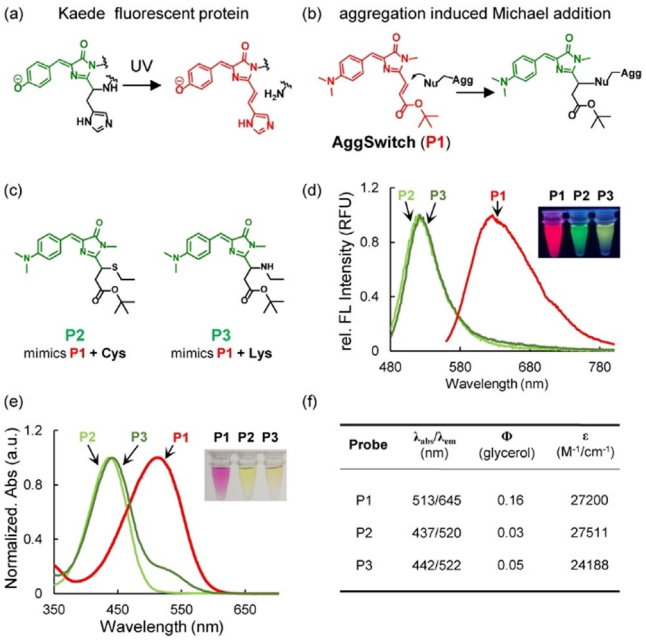

Probe	$\lambda_{abs}/\lambda_{em}$ (nm)	Φ (glycerol)	ε (M^{-1}/cm^{-1})
P1	513/645	0.16	27200
P2	437/520	0.03	27511
P3	442/522	0.05	24188

Figure 2. Bio-inspired fluorescent protein chromophore mimic probe can switch fluorescence color upon Michael addition. a) Kaede fluorescent protein switches its green fluorescence to red upon photolysis. b) Proposed working mechanism of AggSwitch P1 probe. P1 turns on red fluorescence upon binding to misfolded proteins and switches to green fluorescence upon protein aggrega-tion via Michael addition. c) Synthetic P2 and P3 surrogates mimic the Michael addition products of P1 reacting with nucleophilic cysteine (P2) or lysine residues (P3). d) Fluorescence emission spectra of P1, P2, and P3 in glycerol (5.0 μM). e) Absorption spectra of P1, P2, and P3 in methanol (10.0 μM). f) Photo-physical parameters of P1, P2, and P3 in glycerol.

(Figure 2). This probe was bio-inspired and reversely engineered from the chromophore of Kaede photo-convertible fluorescent protein based on its photo-conversion mechanism (Figure 2a). The Kaede fluorescent protein shifts its fluorescent color from green to red upon photolysis. Inspired by this mechanism, our probe P1 (Figure 2b) was designed to bear an electrophilic vinyl ester that is ready for covalent 1, 4-Michael addition by nucleophilic amino acid side chains (Figure 2c, cysteine and lysine). Probe P1 turned on red fluorescence at 645 nm whereas its Michael addition surrogates P2 and P3 exhibited green fluorescence around 520 nm in the viscous glycerol (Figure 2d,f). Meanwhile, the chemical transformation from P1 to P2 and P3 can be reflected by the absorbance spectrum shift upon Michael addition (Figure 2e,f).

Interestingly probe P1, named AggSwitch probe hereafter, remained fluorescently dark when the model protein destabilized *E. coli* dihydrofolate reductase mutant (mut-DHFR, M42T:H114R)[49] was folded (Figure 3a, black curve). Immediately upon acid induced DHFR misfolding and aggregation, we initially observed the occurrence of red fluorescence (Figure 3a, red curve, em_{max} 620 nm, pH 4.4). As the protein aggregation proceeded, the probe gradually changed its fluorescence from red to yellow after 30 min (Figure 3a, yellow curve), and completely switched to green fluorescence after 100 min (Figure 3a, green curve em_{max} 515 nm, $\Phi = 0.07$). As shown in the absorption spectra

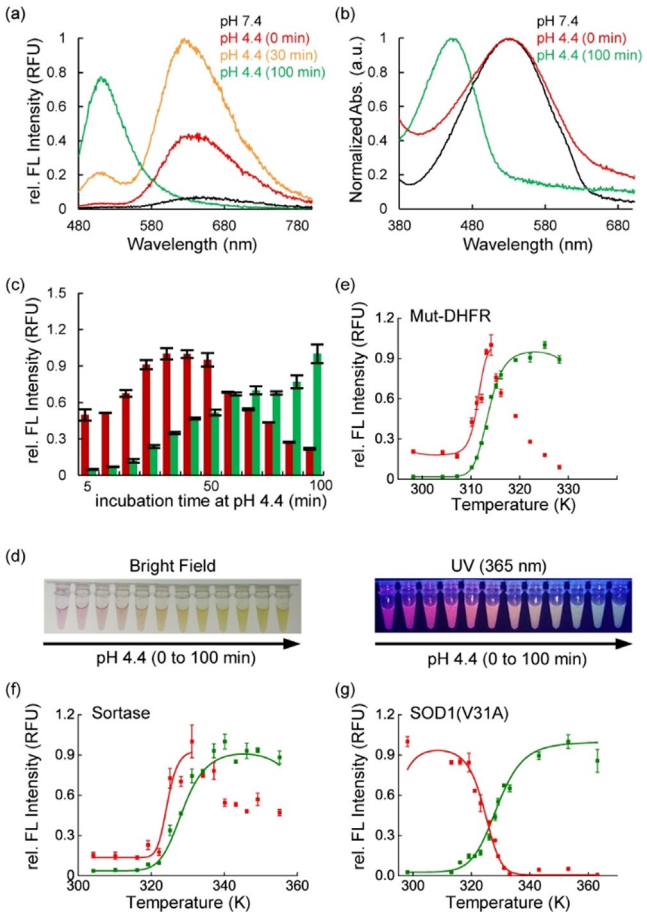

Figure 3. AggSwitch P1 probe is a fluorescent color-switch probe upon protein aggregation. a) Fluorescence spectra of P1 in folded, misfolded, and aggregated mut-DHFR proteins. P1 was dark in folded mut-DHFR (M42T:H114R, 10 μM, pH 7.4), turned on red fluorescence upon acid induced misfolding (pH 4.4, 0 min), and switched to green color after 100 min in acidic buffer (pH 4.4). b) Absorption spectra of P1 in misfolded (red curve) and aggregated (green curve) mut-DHFR. c) Fluorescence of P1 gradually switched from red to green as mut-DHFR misfolded and aggregated induced by acid over time at pH 4.4. d) Images of samples in (c). e) Fluorescence of P1 gradually switched from red to green as heat induced mut-DHFR misfolds and aggregates over time at pH 6.23 from 25 °C to 55 °C. f & g) Fluorescence color-switch property retained in aggregated sortase and SOD1(V31A) proteins.

(Figure 3b), P1 in aggregated proteins shared similar photophysical properties as its Michael addition product P2 and P3, suggesting that such fluorescence color-switch property may be caused by the Michael addition of P1. We further present such fluorescence color-switch property in a time-dependent (Figure 3c) and a temperature-dependent (Figure 3e) protein aggregation experiment. Both experiments confirmed AggSwitch probe first turned on red fluorescence and gradually changed to green fluorescence as mut-DHFR protein aggregated (Figure 3d) but remained non-fluorescent with folded proteins (Figure S1). Finally, we examined the generality of P1's fluorescence color-switch property in different aggregated proteins (sortase in Figure 3f, SOD1(V31A) in 3g, WT-DHFR in Figure S2a). Collectively, we demonstrated that AggSwitch probe (P1) exhibits fluorescence color-switch property as protein misfolds and aggregates.

Michael Addition upon Protein Aggregation

We next attempted to confirm that AggSwitch P1 covalently modified aggregated proteins via Michael addition. Prior to characterizations, we denatured, refolded, and desalted DHFR proteins that were aggregated in the presence of AggSwitch probe (Figure 4a) to minimize the interference from heterogeneous phase separated proteins. We explored series of biochemical and mass spectrometry experiments to examine the presence of covalent modification.

First, the UV/Vis spectrum of the P1-modified refolded proteins (459 nm) shifted towards P2 in MeOH (440 nm)

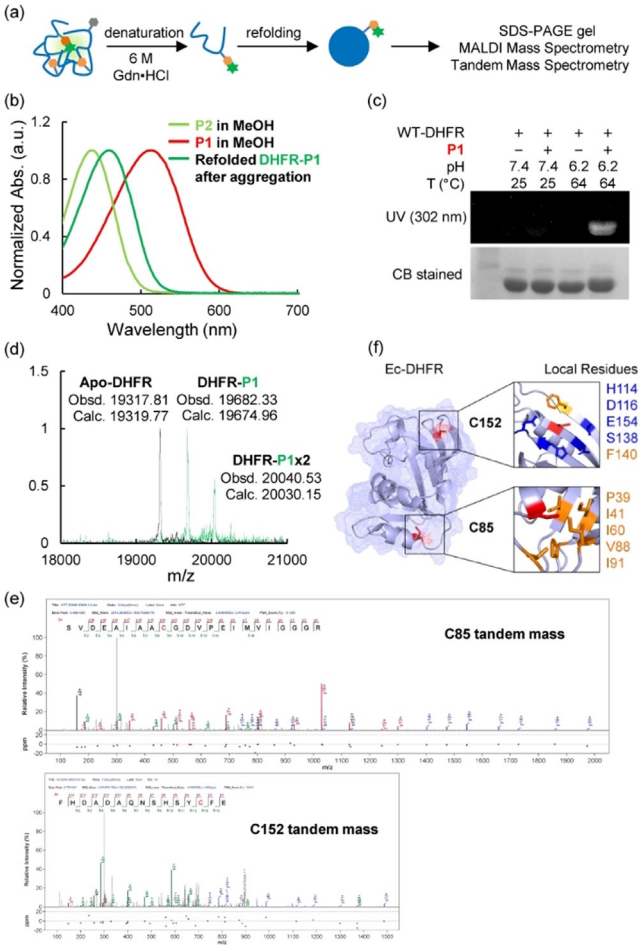

Figure 4. Covalent and chemoselective Michael addition of aggregated proteins by the AggSwitch P1 probe. a) Experimental Scheme to denature and refold aggregated DHFR modified by P1 prior to characterizations. b) Absorption spectra of refolded DHFR aggregates indicated covalent adduct of P1 onto DHFR proteins. c) SDS-Page electrophoresis showed stable covalent adduct of P1 onto DHFR. d) MALDI mass spectrometry identified two covalent modifications by P1 probe on one DHFR protein molecule. e) Tandem mass spectrometry identified C85 and C152 residues that were modified by P1. f) Distinct local environment of C85 and C152 revealed by X-ray crystallography (PDB:5CCC).

compared to P1 in MeOH (513 nm) (Figure 4b). This result indicated that stable covalent Michael addition occurred between the protein and P1 upon DHFR aggregation even after denaturation, refolding, and size exclusion purification to remove non-covalent binders. Second, SDS-PAGE electrophoresis showed that DHFR was covalently modified by a fluorescent probe (Figure 4c for heat induced aggregation, Figure S3 for acid induced aggregation). Third, MALDI mass spectrometry further identified the exact covalent adduct product of DHFR-P1 conjugate, whereas the probe did not modify folded DHFR under the same conditions (Figure 4d, Figure S4). Similar SDS-PAGE gel, MALDI, and color-switch results can be obtained using other model proteins, showing that such Michael addition universally occurs upon protein aggregation (Figure S5, S6). These lines of evidence support that stable covalency present between aggregated DHFR and AggSwitch P1 probe.

We next utilized tandem mass spectrometry to reveal which amino acid residue is responsible for this Michael addition (Figure 4e). Multiple proteases digested aggregated WT-DHFR proteins were subjected to tandem mass spectrometry analysis and showed good peptide coverage (Figure S7). We observed chemoselective conjugation of P1 towards Cysteine-85 (C85) and Cysteine-152 residues (C152) of WT-DHFR protein (Figure 4e, S8). DHFR C85S:C152S double mutant abolished the covalent reaction shown by the MALDI result and the fluorescence color-switch property of P1 upon DHFR aggregation (Figure S9). Furthermore, tandem mass results showed a preferred conjugation towards C85 over C152 (Figure S10, 4.3:1 in labeling efficiency). However, C85 residue of higher labeling efficiency was less exposed to protein surface and thus less accessible to probes than C152 shown by the DHFR X-ray crystallographic structure (Figure 4f, PDB code: 5CCC). We asked why a buried residue was labeled by P1 more effectively than an exposed residue. Scrutinizing the neighboring residues of C85 and C152 revealed their different chemical environment. C85 is buried in a highly hydrophobic environment, whereas C152 is in an exposed charged polar environment (Figure 4f). Therefore, the interaction between hydrophobic C85 pocket and hydrophobic AggSwitch P1 probe ($C\log P = 4.1$) may be more energetically favorable compared to the interaction with hydrophilic C152 pocket due to the hydrophobic effect during protein misfolding and aggregation. This result also depicted that the buried C85 residue first flips inside-out upon protein aggregation, binds P1 probe, and then exposes itself to the probe for Michael addition reaction. Interestingly, cysteines at different locations of DHFR bear different reactivity and reaction kinetics revealed by mutagenesis (Figure S23). Overall, these multiple lines of evidence showed that covalent Michael addition occurs inside aggregated proteins with chemoselectivity to cysteine residues.

Michael Addition Triggers the Fluorescence Color-Switch Property

Protein aggregation is a multi-step phase separation process that involves folded proteins (F), unfolded proteins (U), misfolded soluble oligomers (M), and insoluble aggregates (I) (Figure 5a). We are interested in the origin of individual fluorescent color of P1 and the role of Michael addition in this color-switch behavior. We next attempted to attribute the fluorescence colors of P1 to different protein misfolded states (U, M, and I) and test the proposed mechanisms (Figure 5a).

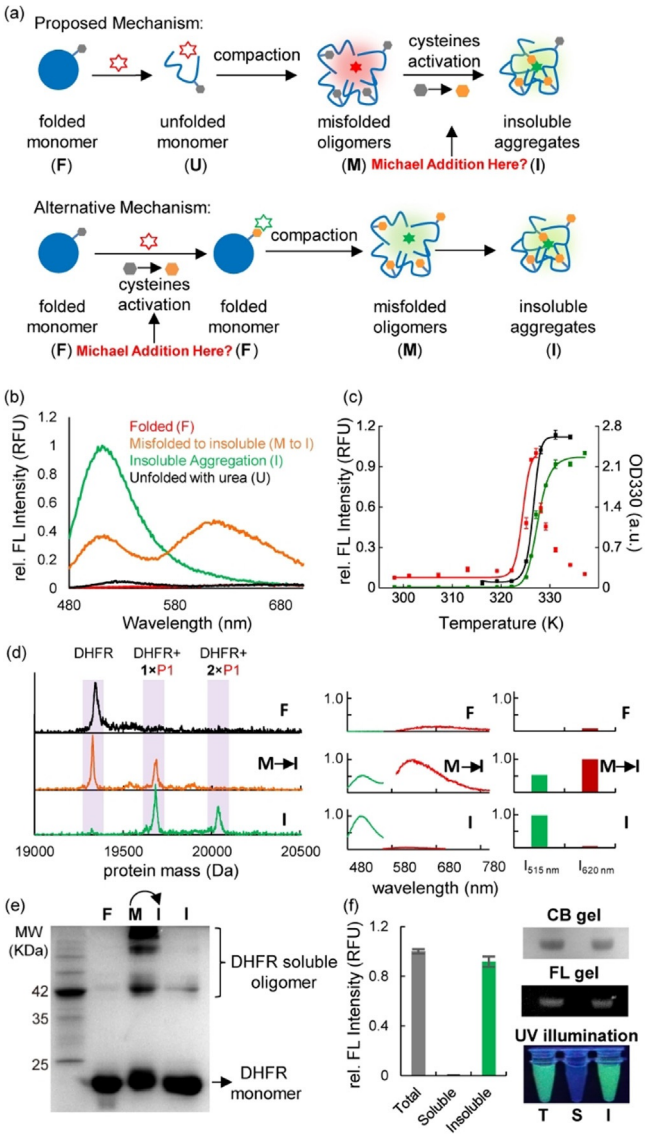

Figure 5. Mechanism of the fluorescence color-switch property of P1. a) Proposed model of stepwise fluorescence turn-on and color-switch upon protein aggregation. P1 is dark in folded and unfolded monomeric proteins (F & U), turns on red fluorescence upon binding to misfolded soluble oligomers (M), and reacts with reactive cysteines upon the formation of insoluble aggregates (I). b) Relative fluorescence intensity of P1 (5 μM) at different folding states of DHFR (50 μM). c) Quantitative thermal shift curves of red fluorescence (red curve), green fluorescence (green curve), and turbidity (black curve). d) MALDI and fluorescence analyses revealed covalent modification triggered the color-switch property. e) Chemical crosslinking experiments revealed red fluorescence is from misfolded soluble oligomers using Coomassie blue stained SDS-PAGE gel. f) Fractionation experiment revealed green fluorescence in the insoluble fraction.

First, urea mediated DHFR protein unfolding resulted in minimal fluorescence increase in neither the red nor the green fluorescence (Figure 5b, black curve). Thus, unfolded proteins are not responsible for the turn-on mechanism of red and green fluorescence. Second, the thermal shift curve of red fluorescence ($T_m = 324.38$ K, Figure 5c, red curve) exhibited a slightly lower melting temperature than that of turbidity assay measuring insoluble aggregates ($T_m = 326.59$ K, Figure 5c, black curve), indicating the red fluorescence might be from misfolded soluble oligomers that formed earlier than the insoluble aggregates of DHFR. Meanwhile, MALDI mass spectrometry result and the corresponding fluorescence profile when DHFR transited from misfolded state to insoluble state (Figure 5d, middle panel, M to I transition state, pH 6.23, 53 °C for 5 min) showed incomplete modification of DHFR proteins by P1 and partial fluorescent conversion from red to green color. Chemical crosslinking of DHFR aggregation intermediates (M to I transition state) confirmed the presence of misfolded soluble oligomeric DHFR (Figure 5e, M to I transition state, Figure S11 for fluorescent gel). The disappearance of DHFR soluble oligomers as protein aggregation proceeded (Figure 5e, I state, pH 6.23, 64 °C for 60 min) matched the decrease in red fluorescence (Figure 5d), again confirming the red fluorescence was from the misfolded oligomeric proteins. Together, these data supported that P1 turned on red fluorescence upon binding to the misfolded soluble oligomers but remained unreacted. Finally, we showed complete conversion of fluorescence from red to green color as aggregated DHFR was all covalently modified by P1 (Figure 5d, lower panel, I state, pH 6.23, 64 °C for 5 min). This result demonstrated color-switch property was triggered by the covalent modification.

Fractionation experiment showed green fluorescence located in the insoluble fraction of aggregated DHFR (Figure 5f, S26), indicating the green fluorescence is from insoluble aggregates of DHFR proteins. Interestingly, AggSwitch P1 probe switched to green fluorescence slightly slower than the formation of DHFR insoluble aggregates shown by the similar melting temperatures in the thermal shift curves of green fluorescence ($T_m = 327.57$ K) and turbidity assay ($T_m = 326.59$ K) (Figure 5c, Figure S2b). This data indicated that the green fluorescence was caused by insoluble DHFR aggregates. It also highlighted the fast labeling kinetics of P1 towards aggregated proteins because no significant delay of green fluorescence from the turbidity data was observed at the given concentrations.

We next explored the impact of covalent linkage on the green fluorescence of P1. P1's Michael addition product surrogate probe P2 without Michael acceptor was not capable of fully turning on the green fluorescence to the same intensity as P1 upon protein aggregation (Figure S12). Furthermore, addition of P1 after the formation of insoluble aggregate protein aggregation could not effectively turn on the green fluorescence either and the reaction is aggregation-stage-depedent (Figure S13). These results indicated that covalency occurring during protein misfolding and aggregation is necessary to fully switch on green fluorescence of P1. Together, these lines of evidence supported a plausible mechanism: AggSwitch probe P1 first binds to misfolded soluble oligomeric proteins via non-covalent physical interactions and turns on its red fluorescence; as proteins form insoluble aggregates, they further compact and activate nucleophiles to react with the probe via Michael addition and switched to the green fluorescence (Figure 5a). The alternative mechanism does not hold true as we observed no covalent modification when protein is folded shown by the MALDI results (Figure 5d) and the presence of red fluorescence during the transition from misfolded oligomers to insoluble aggregates (Figure 5b, c, and d).

Exploiting the Michael Addition Chemistry to Develop Other Protein Aggregation Color-Switch Sensors

To demonstrate this chemistry reported here can be utilized to develop other fluorescence color-switch probes, we designed MG probe (P4) based on the scaffold of malachite green (MG) dye (Figure 6a). MG derivatives have been reported to be fluorogenic upon binding to evolved peptide sequences.[50,51] Thus MG scaffold may inherently bind to aggregated proteins. MG of positive charge possesses electropositivity in the center of the molecule and has been reported as a reversible Michael acceptor with thiol group (Figure S16b).[52] Encouraged by these pieces of evidence, we tested the fluorescence color-switch property of P4 upon the aggregation of mut-DHFR. Surprisingly, we observed exclusively red fluorescence in aggregated mut-DHFR (Figure 6b, $ex._{max}$ 600 nm, $em._{max}$ 652 nm) but no color-switch property as

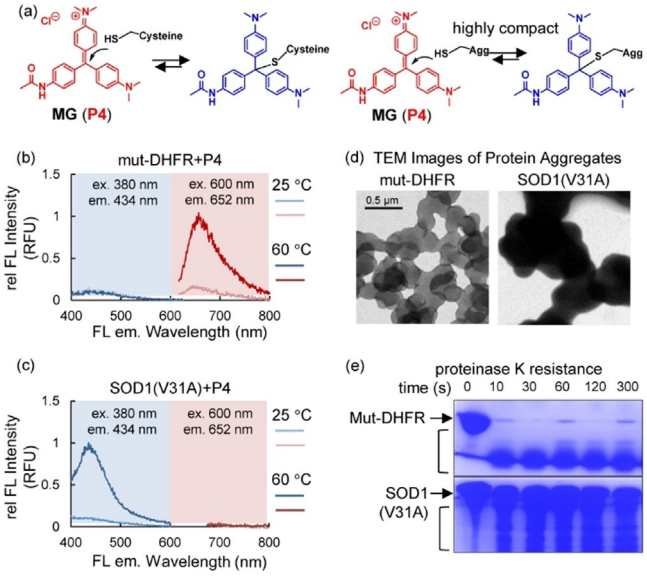

Figure 6. Fluorescent color-switch probe P4 revealed different chemical reactivity inside different protein aggregates. a) Malachite green (MG) dye derivative (P4) can reversibly react with thiols via covalent Michael addition. b) Mut-DHFR's aggregation exclusively turned on the red fluorescence of P4. c) Mutant SOD1 (V31A) switched on the blue fluorescence of P4. d) TEM images of aggregated mut-DHFR and SOD1(V31A) proteins revealed different compactness inside the insoluble aggregates. e) The highly compact SOD1(V31A) aggregates were more resistant to proteolysis than mut-DHFR aggregates.

shown in P1. No fluorescence color-switch responses of P4 towards aggregated DHFR may arise from its decreased chemical reactivity compared to AggSwitch P1 probe because the electropositivity of its Michael acceptor is compromised by the nearby π electrons through electron delocalization. Meanwhile, P4 is also less accessible to nucleophilic conjugation due to its larger steric hindrance than P1. However, fluorescence color-switch property of P4 was resumed when using the other pathogenic model protein mutant superoxide dismutase 1 (SOD1-V31A). We observed exclusively blue fluorescence in aggregated SOD1-V31A (Figure 6c, $ex._{max}$ 380 nm, $em._{max}$ 434 nm).

We then questioned ourselves why P4 exhibited different fluorescence color-switch responses towards different aggregated proteins. Namely why do different aggregated proteins possess differential chemical reactivity? One plausible explanation is that P4 of lower chemical reactivity and higher steric hindrance may require much higher compactness in aggregated proteins in order to bring the probe closer to the reactive nucleophiles for Michael addition. To validate this hypothesis, we first utilized transmission electron microscope to examine the compactness of aggregated DHFR and SOD1 proteins (Figure 6d). We found that aggregated SOD1 is less transparent compared to aggregated DHFR, indicating its higher compactness and density. Second, we used a reported non-covalent protein aggregation sensor AggStain that can detect the local viscosity inside aggregated proteins to reflect its compactness (Figure S14). Supporting the TEM observation, we found aggregated SOD1 is more compact than aggregated DHFR as the sensor exhibited higher fluorescence in aggregated SOD1 (Figure S14). Third, proteolytic resistance of experiment pinpointed that SOD1 aggregate is more compact and less accessible to proteinase K degradation (Figure 6e), which may explain why SOD1 aggregation is pathogenic in vivo but mut-DHFR was reported to be fast degraded. Together, we showed that the compactness of aggregated proteins influences the chemical reactivity of the nucleophiles inside aggregated proteins. The differences of chemical reactivity in aggregated proteins can be reflected by the different fluorescence color-switch response of our probes.

Modulation of the Chemical Reactivity of Michael Addition

The above results suggest that the reactivity of this Michael addition upon protein aggregation is affected by (1) the compactness of aggregated protein and (2) the chemical reactivity of the Michael acceptor in the fluorescent color-switch probe. To further demonstrate the tunability of this chemistry, we then tuned down the chemical reactivity of P4 via enhancing the electron donating capacity, resulting in probe P5 (Figure 7a). Probe P5 of decreased Michael addition reactivity partially converted its red fluorescence to blue fluorescence in SOD1 aggregates (Figure 7b,c), reflecting the compromised reactivity. However, we were not able to observe covalency after denaturing and refolding the aggregated SOD1 in conjugation with P4 and P5 by SDS-PAGE analysis (Figure S15). This is possibly due to the fact that MG

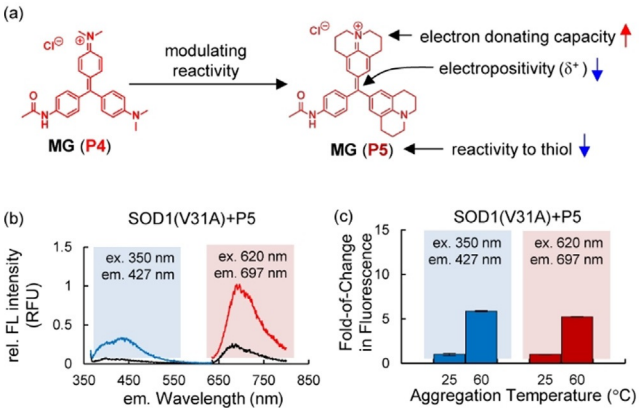

Figure 7. Decreasing MG chemical reactivity leads to partial fluorescence color-switch response to aggregated proteins. a) Decreasing the chemical reactivity of MG dye resulting in P5 probe. b) Emission spectra of P5 in aggregated SOD1(V31A). P5 partially switched its red fluorescence to blue upon SOD1(V31A) aggregated. c) Quantitative analysis of (b).

dye in conjugation with thiol functional group is reversible in both previous study and our experiment (Figure S16b). Overall, these results demonstrated that the Michael addition chemistry upon protein aggregation reported in this work can be modulated by fine-tuning the chemical reactivity of the designed probe. Modulation of chemical reactivity can result in different fluorescence color-switch response towards aggregated proteins.

Michael Addition Reactivity of Cellular Aggregated Proteome

Finally, we examined whether this chemistry can occur in the aggregated proteome of stressed live cells. Supported by the above in vitro results, our proposed Michael addition reaction model is that the probe first selectively binds to misfolded proteins, turns on the red fluorescence, and then switches to green color upon aggregation induced covalent reaction. To examine this model in live cells, proteome aggregation was first induced by attenuating cellular protein degradation using proteasome inhibitor MG132. We attempted to visualize aggregated proteome by confocal microscopy using AggSwitch P1 due to its better spectral alignment with commercial laser source. As expected, we observed punctate and peri-nuclear aggresomes exclusively in the green channel upon addition of proteasome inhibitor MG132 in U251 human glioblastoma cells for 18 h (Figure 8, lower panel), whereas the control cells at basal condition were not fluorescent (Figure 8, upper panel). Fractionation of cellular lysate further confirmed the green fluorescent aggregates formed in the stressed proteome (Figure S18). Interestingly, we observed the intermediate red fluorescence of P1 upon short-term 5 h stress (Figure 8 middle panel), supporting our in vitro model (Figure 5a). In addition, P2 added prior to or after proteome aggregation was not capable of staining aggregated proteome (Figure S17), indicating covalency is required for efficient switch-on of the green fluorescence. This result echoed our in vitro experiment shown in Fig-

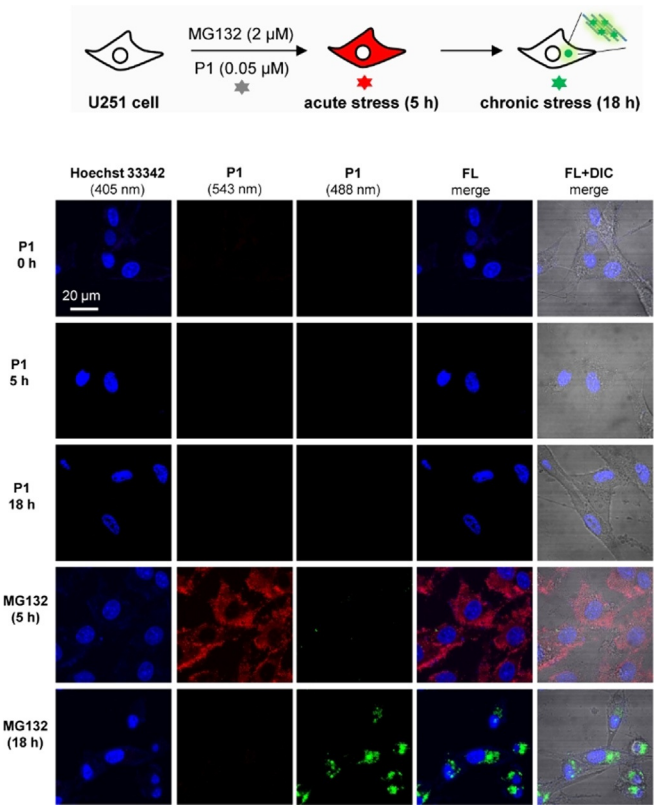

Figure 8. Detecting aggregated proteome in stressed live cells via the Michael addition reaction with AggSwitch P1. Confocal images of U251 cells stressed by MG132 to induce proteome aggregation. Experimental details see Supporting Information.

ure S12. These imaging results suggested that probe P1 is a fluorescent color-switch probe upon protein aggregation induced by Michael addition and can be utilized to detect aggregated proteome in stressed cells.

Discussion on the Design Strategy for Covalent Probes Targeting Aggregated Proteins

What structural features does a probe need to harbor in order to selectively target the reactive nucleophiles in aggregated proteins? Our results highlight three requirements for a designed probe to covalently label aggregated proteins. First, the probe needs to harbor a Michael acceptor or other potential reactive electrophiles for covalent conjugation. Second, the core structure of the designed probe tends to inherently bind misfolded and aggregated proteins in order to bring the probe close enough to the reactive nucleophiles and trigger this chemistry. Third, the protein is not cysteine free if using Michael addition.

Several lines of evidence support these notions. First, the non-covalent analogues of P1 have been reported to exhibit inherent binding affinity towards aggregated proteins and be fluorogenic (Figure S19).[53] Therefore, this core scaffold of P1 serves as a guiding moiety to selectively bind to aggregated proteins. However, without the Michael acceptor functional groups, covalency was not expected to occur and the fluorogenicity was also reversible (Figure S19). Second, P1 itself first turned on its red fluorescence upon protein misfolding, indicating P1 tends to bind misfolded proteins prior to covalent conjugation (Figure 5). We then asked whether all Michael acceptors can label aggregated proteins. To test this hypothesis, we installed the vinyl ester Michael acceptor onto a common BODIPY fluorophore scaffold (M3, Figure S20) that is not an inherent binder for aggregated proteins, resulting in P6 probe. We observed neither covalent labeling of aggregated protein by P6 nor color-switch property (Figure S20). Therefore, even though they harbor a Michael acceptor, probes of no binding affinity to aggregated proteins are not capable of covalent modification. This is probably why such reactivity was not reported previously given the wide applications of Michael acceptor probes. Third, cysteine-free protein, like our DHFR mutant (C85S:C152S, Figure S9), cannot be modified by P1, showing that the protein needs to harbor nucleophilic cysteine for Michael addition to occur. However, reaction with other less nucleophilic residues (lysine or serine) may occur if the electrophile of a probe is more reactive. If a fluorogenic covalent sensor for aggregated proteins was desired for imaging purpose, the scaffold may exhibit polarity or viscosity dependent fluorescence upon binding to aggregated proteins as our P1, P2, P3, P4, and P5 probes (Figure S21, S22).

Thus, a probe bearing inherent binding affinity to aggregated proteins and a Michael acceptor can undergo the Michael addition reaction reported here. The inherent binding capacity of the probe will guide the probe into misfolded proteins first. Upon protein aggregation, protein structurally collapses and compacts to bring the probe and reactive nucleophiles close enough for covalent reaction. However, further elaboration of the scaffold diversity of binding moieties and the chemical reactivity of the warheads is desired to understand how to selectively target the aggregates of specific protein-of-interest.

Conclusion

In summary, we have reported in this work that Michael addition reaction can occur upon protein aggregation. Based on this chemistry, we designed color-switch fluorogenic probes of tunable fluorescence responses towards different protein aggregates. We revealed that different protein aggregates may exhibit different compactness, proteolytic resistance, and consequently chemical reactivity. In the future, exploration of other potential chemical reaction types and precise control over the chemical reactivity upon protein aggregation may lead to novel chemical strategies to target proteins at this challenging folding state. New covalent labeling chemistry of aggregated proteins may offer opportunities to develop functional probes, such as sensors for imaging, activity-based probes for aggregated proteome profiling, and covalent PROTAC[54] or LyTAC[55] drugs for clearance of pathogenic aggregation.

Acknowledgements

This work was supported, in part, by funds National Natural Science Foundation of China (21907091), the LiaoNing Revitalization Talents Program from the Liaoning province of China (XLYC1907048), Dalian Innovation Fund (2020JJ26GX027), China Postdoctoral Science Foundation Grant (2019M661138), the National Key Research and Development Program of China (2017YFA0505003), National Natural Science Foundation (21725506).

Conflict of interest

The authors declare no conflict of interest.

Keywords: bioconjugation · fluorescent probe · fluorescent proteins · protein aggregation · protein chemistry

[1] C. B. Anfinsen, *Science* **1973**, *181*, 223 – 230.
[2] O. Boutureira, G. J. L. Bernardes, *Chem. Rev.* **2015**, *115*, 2174 – 2195.
[3] J. Kalia, R. T. Raines, *Curr. Org. Chem.* **2010**, *14*, 138 – 147.
[4] J. C. Vantourout, S. R. Adusumalli, K. W. Knouse, D. T. Flood, A. Ramirez, N. M. Padial, A. Istrate, K. Maziarz, J. N. DeGruyter, R. R. Merchant, J. X. Qiao, M. A. Schmidt, M. J. Deery, M. D. Eastgate, P. E. Dawson, G. J. L. Bernardes, P. S. Baran, *J. Am. Chem. Soc.* **2020**, *142*, 17236 – 17242.
[5] D. T. Flood, X. J. Zhang, X. Fu, Z. X. Zhao, S. Asai, B. B. Sanchez, E. J. Sturgell, J. C. Vantourout, P. Richardson, M. E. Flanagan, D. W. Piotrowski, D. K. Kölmel, J. Q. Wan, M. H. Tsai, J. S. Chen, P. S. Baran, P. E. Dawson, *Angew. Chem. Int. Ed.* **2020**, *59*, 7377 – 7383; *Angew. Chem.* **2020**, *132*, 7447 – 7453.
[6] R. E. Thompson, A. J. Stevens, T. W. Muir, *Nat. Chem.* **2019**, *11*, 737 – 743.
[7] C. B. Rosen, M. B. Francis, *Nat. Chem. Biol.* **2017**, *13*, 697 – 705.
[8] A. Bandyopadhyay, S. Cambray, J. M. Gao, *J. Am. Chem. Soc.* **2017**, *139*, 871 – 878.
[9] K. C. Li, W. J. Wang, J. M. Gao, *Angew. Chem. Int. Ed.* **2020**, *59*, 14246 – 14250; *Angew. Chem.* **2020**, *132*, 14352 – 14356.
[10] A. Bandyopadhyay, S. Cambray, J. M. Gao, *Chem. Sci.* **2016**, *7*, 4589 – 4593.
[11] T. P. Smith, I. W. Windsor, K. T. Forest, R. T. Raines, *J. Med. Chem.* **2017**, *60*, 7820 – 7834.
[12] B. J. Pinch, Z. M. Doctor, B. Nabet, C. M. Browne, H. S. Seo, M. L. Mohardt, S. Kozono, X. Lian, T. D. Manz, Y. Chun, S. Kibe, D. Zaidman, D. Daitchman, Z. C. Yeoh, N. E. Vangos, E. A. Geffken, L. Tan, S. B. Ficarro, N. London, J. A. Marto, S. Buratowski, S. Dhe-Paganon, X. Z. Zhou, K. P. Lu, N. S. Gray, *Nat. Chem. Biol.* **2020**, *16*, 979 – 987.
[13] B. A. Lanman, J. R. Allen, J. G. Allen, A. K. Amegadzie, K. S. Ashton, S. K. Booker, J. J. Chen, N. Chen, M. J. Frohn, G. Goodman, D. J. Kopecky, L. Liu, P. Lopez, J. D. Low, V. Ma, A. E. Minatti, T. T. Nguyen, N. Nishimura, A. J. Pickrell, A. B. Reed, Y. Shin, A. C. Siegmund, N. A. Tamayo, C. M. Tegley, M. C. Walton, H. L. Wang, R. P. Wurz, M. Xue, K. C. Yang, P. Achanta, M. D. Bartberger, J. Canon, L. S. Hollis, J. D. McCarter, C. Mohr, K. Rex, A. Y. Saiki, T. San Miguel, L. P. Volak, K. H. Wang, D. A. Whittington, S. G. Zech, J. R. Lipford, V. J. Cee, *J. Med. Chem.* **2020**, *63*, 52 – 65.
[14] A. Cuesta, X. Wan, A. L. Burlingame, J. Taunton, *J. Am. Chem. Soc.* **2020**, *142*, 3392 – 3400.
[15] J. S. Cisar, O. D. Weber, J. R. Clapper, J. L. Blankman, C. L. Henry, G. M. Simon, J. P. Alexander, T. K. Jones, R. A. B. Ezekowitz, G. P. O'Neill, C. A. Grice, *J. Med. Chem.* **2018**, *61*, 9062 – 9084.
[16] T. E. Bearrood, G. Aguirre-Figueroa, J. Chan, *Bioconjugate Chem.* **2020**, *31*, 224 – 228.
[17] J. W. Brulet, A. L. Borne, K. Yuan, A. H. Libby, K. L. Hsu, *J. Am. Chem. Soc.* **2020**, *142*, 8270 – 8280.
[18] X. Y. Zhang, V. M. Crowley, T. G. Wucherpfennig, M. M. Dix, B. F. Cravatt, *Nat. Chem. Biol.* **2019**, *15*, 737 – 746.
[19] J. C. Peeler, E. Weerapana, *Acc. Chem. Res.* **2019**, *52*, 2832 – 2840.
[20] J. X. Huang, G. Lee, K. E. Cavanaugh, J. W. Chang, M. L. Gardel, R. E. Moellering, *Nat. Methods* **2019**, *16*, 894 – 901.
[21] C. S. Lentz, J. R. Sheldon, L. A. Crawford, R. Cooper, M. Garland, M. R. Amieva, E. Weerapana, E. P. Skaar, M. Bogyo, *Nat. Chem. Biol.* **2018**, *14*, 609 – 617.
[22] G. Li, J. E. Montgomery, M. A. Eckert, J. W. Chang, S. M. Tienda, E. Lengyel, R. E. Moellering, *Nat. Commun.* **2017**, *8*, 1775.
[23] W. T. Chen, J. J. Dong, L. Plate, D. E. Mortenson, G. J. Brighty, S. H. Li, Y. Liu, A. Galmozzi, P. S. Lee, J. J. Hulce, B. F. Cravatt, E. Saez, E. T. Powers, I. A. Wilson, K. B. Sharpless, J. W. Kelly, *J. Am. Chem. Soc.* **2016**, *138*, 7353 – 7364.
[24] R. E. Moellering, B. F. Cravatt, *Science* **2013**, *341*, 549 – 553.
[25] J. Wang, Y. Liu, Y. J. Liu, S. Q. Zheng, X. Wang, J. Y. Zhao, F. Yang, G. Zhang, C. Wang, P. R. Chen, *Nature* **2019**, *569*, 509 – 513.
[26] J. S. Italia, P. S. Addy, S. B. Erickson, J. C. Peeler, E. Weerapana, A. Chatterjee, *J. Am. Chem. Soc.* **2019**, *141*, 6204 – 6212.
[27] N. Wang, B. Yang, C. Fu, H. Zhu, F. Zheng, T. Kobayashi, J. Liu, S. Li, C. Ma, P. G. Wang, Q. Wang, L. Wang, *J. Am. Chem. Soc.* **2018**, *140*, 4995 – 4999.
[28] R. D. Row, J. A. Prescher, *Acc. Chem. Res.* **2018**, *51*, 1073 – 1081.
[29] R. M. Sebastian, M. D. Shoulders, *Annu. Rev. Biochem.* **2020**, *89*, 529 – 555.
[30] M. Y. Wong, M. D. Shoulders, *Curr. Opin. Chem. Biol.* **2019**, *50*, 80 – 88.
[31] W. E. Balch, R. I. Morimoto, A. Dillin, J. W. Kelly, *Science* **2008**, *319*, 916 – 919.
[32] F. U. Hartl, *Annu. Rev. Biochem.* **2017**, *86*, 21 – 26.
[33] M. Schmidt, S. Wiese, V. Adak, J. Engler, S. Agarwal, G. Fritz, P. Westermark, M. Zacharias, M. Fandrich, *Nat. Commun.* **2019**, *10*, 5008.
[34] A. Aliyan, N. P. Cook, A. A. Marti, *Chem. Rev.* **2019**, *119*, 11819 – 11856.
[35] P. J. Salveson, S. Haerianardakani, A. Thuy-Boun, S. Yoo, A. G. Kreutzer, B. Demeler, J. S. Nowick, *J. Am. Chem. Soc.* **2018**, *140*, 11745 – 11754.
[36] Y. N. Hong, L. M. Meng, S. J. Chen, C. W. T. Leung, L. T. Da, M. Faisal, D. A. Silva, J. Z. Liu, J. W. Y. Lam, X. H. Huang, B. Z. Tang, *J. Am. Chem. Soc.* **2012**, *134*, 1680 – 1689.
[37] W. Fu, C. X. Yan, Z. Q. Guo, J. J. Zhang, H. Y. Zhang, H. Tian, W. H. Zhu, *J. Am. Chem. Soc.* **2019**, *141*, 3171 – 3177.
[38] M. Z. Chen, N. S. Moily, J. L. Bridgford, R. J. Wood, M. Radwan, T. A. Smith, Z. Song, B. Z. Tang, L. Tilley, X. Xu, G. E. Reid, M. A. Pouladi, Y. Hong, D. M. Hatters, *Nat. Commun.* **2017**, *8*, 474.
[39] M. J. Roberti, M. Morgan, G. Menendez, L. I. Pietrasanta, T. M. Jovin, E. A. Jares-Erijman, *J. Am. Chem. Soc.* **2009**, *131*, 8102 – 8107.
[40] X. P. He, Q. Deng, L. Cai, C. Z. Wang, Y. Zang, J. Li, G. R. Chen, H. Tian, *ACS Appl. Mater. Interfaces* **2014**, *6*, 5379 – 5382.
[41] Y. R. Huang, H. J. Cho, N. Bandara, L. Sun, D. Tran, B. E. Rogers, L. M. Mirica, *Chem. Sci.* **2020**, *11*, 7789 – 7799.
[42] B. Jiang, A. Aliyan, N. P. Cook, A. Augustine, G. Bhak, R. Maldonado, A. D. S. McWilliams, E. M. Flores, N. Mendez, M. Shahnawaz, F. J. Godoy, J. Montenegro, I. Moreno-Gonzalez, A. A. Marti, *J. Am. Chem. Soc.* **2019**, *141*, 15605 – 15610.

[43] Y. Liu, C. H. Wolstenholme, G. C. Carter, H. Liu, H. Hu, L. S. Grainger, K. Miao, M. Fares, C. A. Hoelzel, H. P. Yennawar, G. Ning, M. Du, L. Bai, X. Li, X. Zhang, *J. Am. Chem. Soc.* **2018**, *140*, 7381 – 7384.
[44] C. H. Wolstenholme, H. Hu, S. Ye, B. E. Funk, D. Jain, C. H. Hsiung, G. Ning, Y. Liu, X. Li, X. Zhang, *J. Am. Chem. Soc.* **2020**, *142*, 17515 – 17523.
[45] T. C. Owyong, P. Subedi, J. Deng, E. Hinde, J. J. Paxman, J. M. White, W. Chen, B. Heras, W. W. H. Wong, Y. Hong, *Angew. Chem. Int. Ed.* **2020**, *59*, 10129 – 10135; *Angew. Chem.* **2020**, *132*, 10215 – 10221.
[46] A. K. Yadav, C. J. Reinhardt, A. S. Arango, H. C. Huff, L. Dong, M. G. Malkowski, A. Das, E. Tajkhorshid, J. F. Chan, *Angew. Chem. Int. Ed.* **2020**, *59*, 3307 – 3314; *Angew. Chem.* **2020**, *132*, 3333 – 3340.
[47] S. H. Gardner, C. J. Reinhardt, J. F. Chan, *Angew. Chem. Int. Ed.* **2021**, *60*, 5000 – 5009; *Angew. Chem.* **2021**, *133*, 5052 – 5062.
[48] A. K. East, M. Y. Lucero, J. Chan, *Chem. Sci.* **2021**, *12*, 3393 – 3405.
[49] L. A. Banaszynski, L. C. Chen, L. A. Maynard-Smith, A. G. L. Wandless, T. J. Ooi, *Cell* **2006**, *126*, 995 – 1004.
[50] C. Szent-Gyorgyi, B. F. Schmidt, Y. Creeger, G. W. Fisher, K. L. Zakel, S. Adler, J. A. Fitzpatrick, C. A. Woolford, Q. Yan, K. V. Vasilev, P. B. Berget, M. P. Bruchez, J. W. Jarvik, A. Waggoner, *Nat. Biotechnol.* **2008**, *26*, 235 – 240.
[51] T. M. Ayele, S. D. Knutson, S. Ellipilli, H. Hwang, J. M. Heemstra, *Bioconjugate Chem.* **2019**, *30*, 1309 – 1313.
[52] D. M. E. Reuben, T. C. Bruice, *J. Am. Chem. Soc.* **1976**, *98*, 114 – 121.
[53] W. Wan, W. Jin, Y. Huang, Q. Xia, Y. Bai, H. Lyu, D. Liu, X. Dong, W. Li, Y. Liu, *Anal. Chem.* **2021**, *93*, 1717 – 1724.
[54] G. M. Burslem, C. M. Crews, *Cell* **2020**, *181*, 102 – 114.
[55] S. M. Banik, K. Pedram, S. Wisnovsky, G. Ahn, N. M. Riley, C. R. Bertozzi, *Nature* **2020**, *584*, 291 – 297.

Manuscript received: December 1, 2020
Revised manuscript received: February 4, 2021
Accepted manuscript online: March 2, 2021
Version of record online: April 9, 2021

